THE JOURNAL OF BIOLOGICAL CHEMISTRY
Vol. 276, No. 35, Issue of August 31, pp. 32575–32584, 2001

Printed in U.S.A.

Three-dimensional Interaction of Phi29 pRNA Dimer Probed by Chemical Modification Interference, Cryo-AFM, and Cross-linking*

Received for publication, January 3, 2001, and in revised form, May 17, 2001
Published, JBC Papers in Press, May 22, 2001, DOI 10.1074/jbc.M100045200

Yahya Mat-Arip‡§¶, Kyle Garver‡¶‖, Chaoping Chen‡§§, Sitong Sheng‡‡, Zhifeng Shao‡‡, and Peixuan Guo‡

From the ‡Department of Pathobiology, Purdue University, West Lafayette, Indiana 47907 and the ‡‡Department of Molecular Physiology and Biological Physics, University of Virginia, Charlottesville, Virginia 22908

Six pRNAs (p for packaging) of bacterial virus phi29 form a hexamer complex that is an essential component of the viral DNA translocating motor. Dimers, the building block of pRNA hexamer, assemble in the order of dimer → tetramer → hexamer. The two-dimensional structure of the pRNA monomer has been investigated extensively; however, the three-dimensional structure concerning the distance constraints of the three stems and loops are unknown. In this report, we probed the three-dimensional structure of pRNA monomer and dimer by photo affinity cross-linking with azidophenacyl. Bases 75–81 of the left stem were found to be oriented toward the head loop and proximate to bases 26–31 in a parallel orientation. Chemical modification interference indicates the involvement of bases 45–71 and 82–91 in dimer formation. Dimer was formed via hand-in-hand contact, a novel RNA dimerization that in some aspects is similar to the kissing loops of the human immunodeficiency virus. The covalently linked dimers were found to be biologically active. Both the native dimer and the covalently linked dimer were found by cryo-atomic force microscopy to be similar in global conformation and size.

Interactions between RNA molecules play diverse roles in different biological systems. Dimerization of retrovirus RNAs via kissing loops is believed to govern essential steps in the retroviral life cycle, including translation, reverse transcription, RNA encapsidation, and virion assembly (1, 2). During the early events of pre-mRNA splicing, there are several types of interactions through a network of RNA-RNA, RNA-protein, and protein-protein contacts (3–6). In addition, RNA-RNA interactions are also involved in the cleavage of tRNA by RNase P (7–9), and in genetic regulations in bacteria (10, 11), eukaryotes (12), plants (13), mammals (14), and plasmids (15).

An intermediate step in morphogenesis of phi29, a bacterial virus that infects *Bacillus subtilis*, is the formation of a DNA-filled capsid generated through the translocation of genomic dsDNA into an empty capsid shell (procapsid or prohead), a process called DNA packaging (for reviews, see Ref. 16). Translocation of double-stranded DNA into the procapsid requires a pair of noncapsid proteins and a virus-encoded RNA (17, 18), called pRNA[1] (p for packaging). The 120-base pRNA participates in the DNA packaging reaction but is not a part of the mature phi29 virion. The pRNA binds to the connector (the unique site where DNA goes through) of procapsids in the presence of Mg^{2+} (19). The pRNA also appears to be directly involved in the DNA translocation process and leaves the procapsid after DNA packaging is completed (20).

To elucidate the role of the pRNA in this DNA translocating motor, it is crucial to know how many copies of the pRNA are involved in each DNA packaging event. We have developed three approaches to determine the stoichiometry of the pRNA. These three approaches have led to the conclusion that six pRNAs are required for the function of each motor.

The first determination of pRNA stoichiometry involved the use of binomial distribution (21, 22). pRNAs with mutations in the 5′/3′ paired region (the DNA translocation domain) retained procapsid binding capacity but failed to package DNA. When mutant pRNA and wild-type pRNA were mixed at various ratios in *in vitro* assembly assays, the probability of procapsids that possess a certain amount of mutant and a certain amount of wild-type pRNA was determined by the expansion of a binomial $(p + q)^Z$, where Z is the total number of pRNA per procapsid, and p and q represent the percent of mutant and wild-type pRNA, respectively, used in reaction mixtures. For example, if we assume that Z is 3, the probability of all combinations of mutant and wild-type pRNAs on a given procapsid can be predicted by the expansion of the binomial: $(p + q)^3 = p^3 + 3p^2q + 3pq^2 + q^3 = 100\%$. The yield of virions from empirical data was plotted and compared with a series of predicted curves to find a best fit. Our results showed that approximately five to six pRNAs were needed for each procapsid to package DNA, explaining the high inhibition efficiency of mutant pRNA (23).

The second approach for stoichiometry determination utilized serial dilution factor of pRNA *versus* the yield of virions assembled *in vitro* (21). The larger the stoichiometry of the component, the more dramatic the influence of the dilution

* This work was supported by National Institutes of Health Grants GM59944 (mainly) and GM60529 (to P. G.) and by National Institutes of Health Grant RR07720 (to Z. S.). The costs of publication of this article were defrayed in part by the payment of page charges. This article must therefore be hereby marked "*advertisement*" in accordance with 18 U.S.C. Section 1734 solely to indicate this fact.

§ Supported by a fellowship from the Universiti Sains Malaysia.

¶ These two authors contributed equally to this paper. Both of them can be regarded as the first author of this article.

‖ Current address: Western Fisheries Research Center, 6505 NE 65th St., Seattle, WA 98115.

** To whom correspondence should be addressed: Purdue Cancer Research Center, B-36 Hansen Life Science Research Bldg., Purdue University, West Lafayette, IN 47907. Tel.: 765-494-7561; Fax: 765-496-1795; E-mail: guo@vet.purdue.edu.

§§ Current address: Dept. of Molecular Genetics and Biochemistry, University of Pittsburgh Medical School, Pittsburgh, PA 15261.

[1] The abbreviations used are: pRNA, packaging RNA; AFM, atomic force microscopy; PCR, polymerase chain reaction; DMS, dimethyl sulfate; DEPC, diethyl pyrocarbonate; CMCT, (1-cyclohexyl-3-(2-morpholinoethyl)carbodiimide metho-*p*-toluene sulfonate); cp-pRNA, circularly permuted pRNA; APA, azidophenacyl; PAGE, polyacrylamide gel electrophoresis.

TABLE I
Oligonucleotides

Designation	Sequence	Size	Location (residues)
5′ T7–75	5′ TAATACGACTCACTATAGTTGATTGGTTGTCAAT 3′	34	75–91
3′ P71	5′ GTATGTGGGCTGAACTCAATCAGGG 3′	25	71–47
5′ SP6–78	5′ ATTTAGGTGACACTATAGATTGGTTGTCAATCAT 3′	34	78–94
3′ P77	5′ AACAAAGTATGTGGGCT 3′	17	77–61
5′ T7–108	5′ TAATACGACTCACTATAGCTACTTTCCTAAAGGAA 3′	35	108–4
3′ P107	5′ GGCACTTTTGCCACGATTGA 3′	20	107–87
P7	5′ TAATACGACTCACTATAGCAATGGT 3′	25	1–10
P11	5′ TTAGCAAAGTAGCGTGCACTTTTG 3′	24	120–96
5′ G^{23}	5′ TAATACGACTCACTATAGGTCATGTGTATGTTGGG 3′	35	23–39
3′ C^{97}b′	5′ GCCATGATTGACACGCAATC 3′	20	97–78
P103–82	5′ ACTTTTGCCATGATTGACGGACA 3′	23	103–81

factor on the reaction. A slope of one indicates that one copy of the component is involved in the assembly of one virion. A slope larger than one would indicate multiple-copy involvement. Our result of log plots dilution factor *versus* virions assembled support the conclusion that the stoichiometry of pRNA in DNA packaging is between five and six.

The stoichiometry of pRNA was also investigated by the mixing together of inactive mutant pRNAs, each having interactive complementary loops, in DNA packaging reactions to determine the common multiples (24, 25). Since infectious virions could be produced by mixing two inactive pRNAs with interlocking loops, we showed that the stoichiometry of the pRNA is a multiple of two (24, 25). Likewise, since infectious virions could also be produced by mixing together another set of three inactive pRNAs with interlocking loops, we showed that the stoichiometry of the pRNA is also a multiple of three. Therefore, we confirmed that the stoichiometry of pRNA in DNA packaging is the common multiple of 2 and 3, that is, 6 or 12. Together with the results from binomial distribution and serial dilution analyses (23, 71), we confirmed that the stoichiometry of pRNA was six.

The requirement of six pRNAs in phi29 DNA packaging is supported by the finding that a pRNA dimer is the building block in the assembly of pRNA hexamers (26). We found that the sequence in the assembly of hexamers is dimer → tetramer → hexamer. The low resolution three-dimensional structure of pRNA monomers and dimers has been shown by cryo-atomic force microscopy (26, 27). Monomers exhibit a "check mark" shape, while the dimer displays an elongated shape, with a size approximately twice as long as the monomer (27).

The finding that phi29 RNA forms hexamers as part of an ATP-driven DNA translocation machinery (24, 25, 28) has suggested commonalties between viral DNA packaging and other universal DNA/RNA-tracking/riding processes, including DNA replication (29) and RNA transcription (24, 30). The DNA/RNA-tracking/riding enzymes include helicases (31–34), enhancers (35), *Escherichia coli* transcription terminator Rho (36), yeast PCNA, and DNA polymerase III holoenzyme (37), each of which also forms a hexameric complex or shape. Viral DNA packaging, cellular DNA replication, and RNA transcription are all involved in the relative movement of two components, one of which is nucleic acid. It would be intriguing to show how the phi29 pRNA may play a role that is similar to that of protein enzymes. It is speculated that transportation of macromolecules by RNA complex, assembled via intermolecular lop/loop interaction, exists in the life cycle of eukaryotic cell differentiation (38).

We have determined the pathways and conditions for the assembly of functional pRNA hexamers, where dimers serve as the building blocks (26). In this study, the three-dimensional structure of the monomer and the dimer was probed by chemical modification interference, site-specific photoaffinity cross-linking, and cryo-AFM. This paper provides a first report of pRNA three-dimensional structural constraints.

EXPERIMENTAL PROCEDURES

Synthesis and Purification of pRNAs—pRNAs were prepared as described before (39–41). Briefly, plasmid DNA was used as a template for polymerase chain reaction (PCR) to prepare DNA templates for *in vitro* transcription reaction. The primers used to produce DNA template, as well as reverse transcriptase primer extension, are listed in Table I. The PCR products were purified using Qiaex II (Qiagen, Inc.) and made ready for transcription with a T7 Ribomax transcription kit (Promega, Inc.). Preparation of covalently linked dimer has been described previously (26).

After synthesis, pRNAs were treated with RNase-free DNase I and then subjected to 8 M urea, 8% polyacrylamide gel electrophoresis. Bands of correct size visualized by UV shadow were excised from the gel, and the RNA was eluted overnight at 37 °C in 0.5 M ammonium acetate, 0.1% SDS, 0.1 mM EDTA. After elution, the pRNAs were ethanol-precipitated, washed with 70% ethanol, and resuspended in nuclease-free H_2O. Secondary structure predictions for the pRNA were made using the method of Zuker (42).

Chemical Modification Interference (72)—Two pRNAs 5′/3′ B-a′ and 23/97 A-b′ (Fig. 1) were used to produce dimer (41). However, only pRNA 5′/3′ B-a′ was modified by chemicals. In addition, primers used in reverse transcriptase primer extension were specific to pRNA 5′/3′ B-a′ only. This strategy was to avoid ambiguity primer extension results.

DMS—Purified pRNA (15 pmol) was incubated in buffer D (50 mM sodium cacodylate, pH 7.0, 10 mM $MgCl_2$, 100 mM NaCl) in a final volume of 50 μl. One μl of DMS (diluted 1:3 in 100% ethanol) was added to the reaction. Unmodified control RNA was prepared by including 1 μl of 100% ethanol in the reaction instead of DMS. The reactions were incubated for 3 min at 37 °C. Reactions were stopped by the addition of 6.5 μl of DMS stop buffer (1.0 M Tris acetate, pH 7.5, 1.0 M 2-mercaptoethanol, 1.5 M sodium acetate, 0.1 mM EDTA) and then incubated on ice for 10 min (43).

Reaction volumes were brought up to 200 μl with DEPC-treated water and extracted once with an equal volume of phenol:chloroform: isoamyl alcohol (25:24:1) and once with an equal volume of chloroform: isoamyl alcohol (24:1), followed by ethanol precipitation at −20 °C for several hours. Alternatively, the reactions were ethanol-precipitated directly after termination of the reaction. Pelleted RNA was resuspended in 8 μl of DEPC-treated water.

CMCT—Purified pRNA (15 pmol) in buffer C (50 mM sodium borate, pH 8.0, 20 mM magnesium acetate, 100 mM NaCl) at a final volume of 25 μl was mixed with 25 μl of CMCT (12 mg/ml in buffer C). For unmodified control RNAs, 25 μl of buffer C was added instead of CMCT. Reactions were incubated for 30 min at 37 °C and phenol-extracted and/or ethanol-precipitated as described for DMS modification.

Isolation of Top and Bottom Band—1.5 μl of DMS or 25 μl of CMCT at a concentration of 37 mg/ml was used to modify pRNA 5′/3′ B-a′. The modified pRNA was subjected to electrophoresis in 8 M urea, 8% polyacrylamide gel in TBE (89 mM Tris borate, 2 mM EDTA, pH 8.0) buffer (39, 41). The band was excised using UV shadow and passively eluted overnight at 37 °C in the elution buffer, followed by ethanol precipitation. The modified pRNA was washed with 70% ethanol, and the pellet was resuspended in DEPC-treated water.

An equal molar ratio of the modified pRNA was mixed with pRNA 23/97 A-b′ in TBM (89 mM Tris borate, 5 mM $MgCl_2$, pH 7.6) buffer. The mixture was then run on 8% TBM polyacrylamide gel at 100 volts at

TABLE II
Analysis of crosslinked pRNA species

pRNA[a]	Photo-agent attachment site	Activity		DNA packaging[d]	Cross-linked nucleotides[e]
		Efficiency of cross-link[b]	Procapsid binding[c]		
				pfu/ml	
Wild-type pRNA			+	5.5×10^6	
Cp-pRNA 75/71	G^{75}		+	4.5×10^6	
apa75–1	|	16.9	+	2.3×10^4	ND
apa75–2		18.4	+	1.6×10^4	A^{26}, U^{27}, G^{28}, U^{29}, G^{30}
Cp-pRNA 78/77	G^{78}		+	3.1×10^6	
apa78–1	|	13.7	+	7.5×10^4	ND
apa78–2		16.2	+	8.1×10^4	U^{31}
Cp-pRNA 108/107	G^{108}		+	6.3×10^6	
apa108–1	|	10.7	+	2.0×10^3	ND
apa108–2		8.2	+	1.1×10^3	C^{10}, G^{11}

[a] Individual cross-linked species are designated numerically beginning with the species migrating most slowly in the gel (for example, cross-linked species detected using cp-pRNA 75/71 are denoted apa75–1 and apa75–2).
[b] Efficiency indicates percent conversion to cross-linked species.
[c] Relative procapsid binding indexes are displayed with a "+" indicating that the procapsid binding activity of the cp-RNAs was close to or equal to wild-type pRNA.
[d] Concentration of cross-linked cp-pRNA species was identical to that of its uncross-linked control.
[e] ND, not determined.

4 °C. Gel was stained with ethidium bromide for visualization. Top and bottom bands were excised and passively eluted at 4 °C in the elution buffer, precipitated by ethanol, and resuspended in DEPC-treated water. The top and bottom bands were dialyzed against TE (10 mM Tris-HCl, 1 mM EDTA, pH 8.0) for 1 h before being used in primer extension.

Preparation of Photoagent-containing Circularly Permuted pRNAs (cp-pRNAs)—Guanosine 5′-phosphorothioate-containing cp-pRNAs were prepared by *in vitro* transcription of DNA templates with T7 RNA polymerase in the presence of 40 mM Tris-HCl, pH 7.5, 12 mM $MgCl_2$, 2 mM spermidine, 10 mM NaCl, 1 mM ATP, 1 mM CTP, 1 mM UTP, 0.2 mM GTP, [α-^{32}P]GTP, 8 mM guanosine 5′-phosphorothioate, at 37 °C for 4 h. Transcripts were purified by electrophoresis through 8% polyacrylamide, 8 M urea gels, viewed by autoradiography, and passively eluted into 10 mM Tris-HCl, pH 8, 0.3 M sodium acetate, 1 mM EDTA, and 0.1% SDS. Transcripts were ethanol-precipitated and dried *in vacuo*. Transcripts containing the 5′-terminal phosphate of 5′-guanosine monophosphorothioate were coupled to an azidophenacyl group (44).

Cross-linking—For cross-linking, the conjugated cp-pRNA was incubated in TMS (50 mM Tris-HCl, pH 7.8, 10 mM $MgCl_2$, 100 mM NaCl) and then exposed to UV light (Phillips, UVB 20W-TL01, 311 nm) for 10–20 min at 0 °C. Under these conditions, no photoagent-independent cross-links were detected. The efficiency of intramolecular cross-links (Table II) was measured as a fraction of the total input azido-pRNA using densitometric readings of individual intramolecular cross-linked bands.

Separation of Cross-links by Sucrose Gradient Sedimentation—To separate intermolecular from intramolecular (monomeric) cross-links, linear 5–20% sucrose gradients were prepared in TB (50 mM Tris-HCl, pH 7.6, 89 mM boric acid) buffer. Purified cross-linked species were loaded onto the top of the gradient and spun at 50,000 rpm for 15 h at 4 °C in a SW55 rotor. As sedimentation markers, both pRNA dimers and monomers were run on identical gradients. After sedimentation, fractions were collected at 12 drops each and subjected to scintillation counting.

In Vitro Phi29 Virion Assembly Assay—The purification of procapsids (18, 45, 46), gp16, DNA-gp3 (47); the preparation of neck and tail proteins (48, 49); and the assembly of infectious phi29 virion *in vitro* (48–50) have been described previously.

Reverse Transcriptase Primer Extension—RNA (1.5 pmol) was mixed with 0.1 pmol of γ-^{32}P-end-labeled primer and heated to 90 °C for 2 min. The mixtures were cooled to 30 °C in a water bath (~1 h). RNA/primer mixtures were mixed with 0.5–1 unit of avian myeloblastosis virus reverse transcriptase (Promega), 1 μl of dNTPs (10 mM each), and 2 μl of 5× RT buffer (250 mM Tris-HCl, pH 7.9, 30 mM $MgCl_2$, 10 mM spermidine, 50 mM NaCl) in a final volume of 10 μl. Reactions were incubated at 55 °C for 30 min and stopped by the addition of an equal volume of 2× loading buffer (98% formamide, 10 mM EDTA, 0.01% bromphenol blue, 0.01% xylene cyanol). Samples were heated to 90 °C for 2 min and placed on ice before electrophoresis. Samples were subjected to sequencing-type polyacrylamide gel electrophoresis, and dideoxy sequencing lanes were run adjacent to experimental chemical modification reactions to facilitate mapping of individual bases.

For cross-linked products, individual 5′-^{32}P-labeled oligonucleotide primers targeting various regions of the cp-pRNAs were hybridized to varying amounts of purified intramolecular cross-link species (75 °C, 2 min, then slowly cooled over 10 min to 37 °C). Oligonucleotides were extended by avian myeloblastosis virus reverse transcriptase at 45 °C for 20 min.

Cryo-AFM of pRNA Oligomers—The procedure for cryo-AFM pRNA image analysis has been reported previously (26, 27). The oligomeric pRNAs were purified from native PAGE gel. Briefly, to prepare the sample for cryo-AFM imaging, a piece of mica was freshly cleaved and soaked with spermidine. Excess spermidine was removed by repeated rinses with deionized water. A pRNA sample (10 μg/ml) was applied to mica preincubated with TBM buffer. After 30 s, the unbound pRNA was removed by rinsing with the same buffer. Before the sample was transferred to cryo-AFM for imaging, it was quickly rinsed with deionized water (<1 s), and the solution was removed with dry nitrogen within seconds (51). All cryo-AFM images were collected at 80 K, as described elsewhere (52). Scan lines were removed by an offline matching of the basal line. Calibration of the scanner was performed with mica and 1-μm dot matrix.

RESULTS

Photoaffinity Cross-linking Strategy of pRNA Monomer Using cp-pRNA—Circular permutation allows the introduction of new 5′/3′ termini of pRNA while maintaining the correct folding of RNA molecule (40, 53, 54). Two tandem pRNA coding sequences separated by a three-base sequence were cloned into a plasmid (40, 55). PCR primer pairs complementary to various locations within the tandem pRNA coding sequences were designed to synthesize PCR fragments for transcription of cp-pRNA. We have shown that nonessential bases or their adjacent bases can be used as new termini for constructing active cp-pRNA. The circular permutation system greatly facilitates the construction of mutant pRNA via PCR and the labeling of any specific internal base by radioactive or photoaffinity agents (Fig. 1).

We performed photo-affinity cross-linking by attaching a photosensitive agent to the 5′-end of the pRNA. The locations of the new end points in cp-pRNAs used in this analysis were selected primarily due to their ability to maintain wild-type activity as well as for their strategic positions in the secondary structure (40, 55, 56). One of the sites is located within the terminal helix necessary for DNA packaging, while two of the other sites chosen are located within interior sequences involved in procapsid binding. It was expected that data from these constructs would provide structural information regarding the two functional domains and their position relative to one another within the pRNA. It has been reported that cp-pRNAs form the native structure, while the 5′ and 3′-ends are

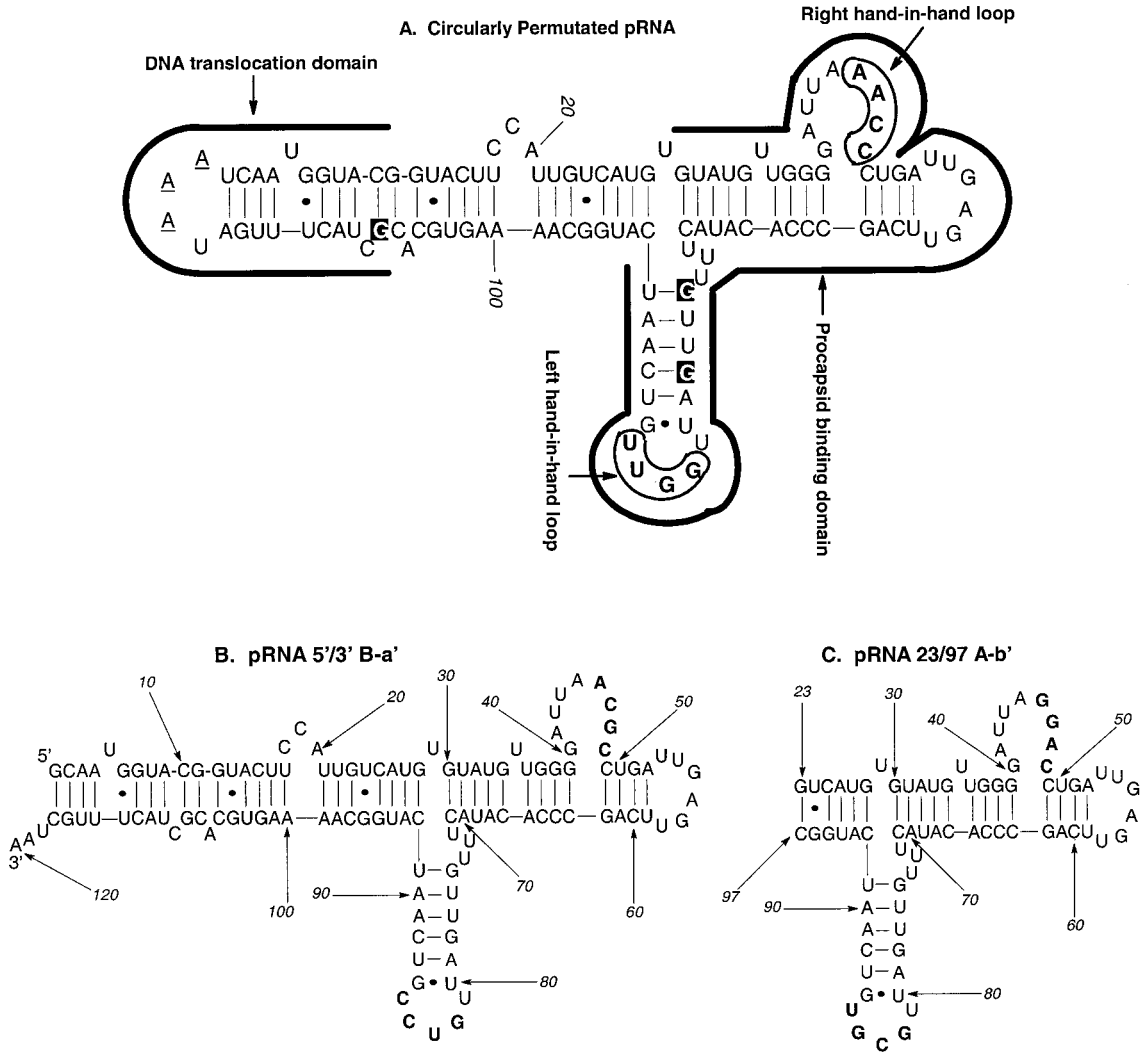

FIG. 1. **Secondary structure of circularly permutated pRNA and the locations of photoagent attachment sites indicated by filled boxes (*A*).** The numbering of pRNA is that of the native sequence. Non-native nucleotides included in the circularly permuted pRNA are the three A's *underlined*. The procapsid binding domain and the DNA translocation domain are marked with *bold lines*, and the four bases in the *right* and *left loops* responsible for inter-RNA interactions are *boxed* and in *bold*. Secondary structure of pRNA 5′/3′ B-a′ (*B*) and pRNA 23/97 (*C*), which interact intermolecularly to form dimer are shown. The truncated pRNA 23/97 was shown to be the smallest molecule that able to retain dimerization (41).

relocated (40). Nevertheless, it was important that the cp-pRNAs studied here reflect the native pRNA structure accurately. Previous analysis of the three cp-pRNAs chosen for this study has revealed that these cp-pRNAs possess both wild-type procapsid binding and DNA packaging activity (40, 55).

Cross-linking of Photoagent-modified cp-pRNA Monomers—For cross-linking, an azidophenacyl (APA) group was attached to the 5′-end of individual cp-pRNAs. For the 5′ modification, the APA group was attached to cp-pRNAs containing a 5′-phosphorothioate incorporated during transcription (44). Inclusion of guanosine monophosphorothioate in transcription reactions results in its incorporation only at the 5′-end, because nucleoside monophosphates can initiate transcription, but are unable to be utilized for elongation by T7 RNA polymerase. The phosphorothioate sulfur provides a unique site on RNA for the attachment of the azidophenacyl group. The photoaffinity-modified cp-pRNAs are subsequently UV-irradiated, thus converting the azido group to a highly reactive nitrene and able to insert into a variety of covalent bonds. An APA derivative was used to provide long range cross-links to identify proximal regions within or between structural motifs.

To monitor the cross-linking reactions, UV-treated photoagent-modified cp-pRNAs were resolved on denaturing polyacrylamide gels (PAGE). The cross-linked species appeared as bands migrating more slowly than uncross-linked RNA (Fig. 2). As in previous analysis (56), cross-linking occurred exclusively

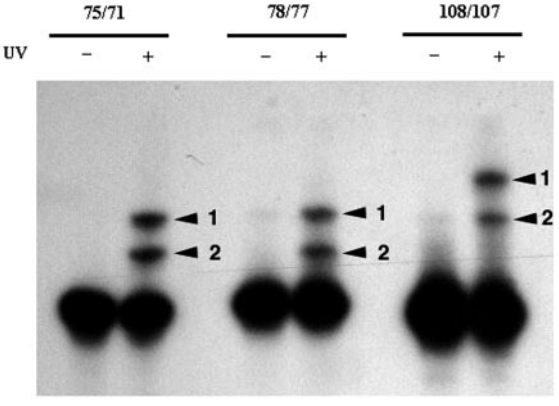

FIG. 2. **Identification of cross-linked species.** Radiolabeled 5′-APA cp-pRNAs were untreated (−) or treated (+) with 311 nm light for 15 min. Cross-linked species, and uncross-linked RNA were resolved on a denaturing polyacrylamide gel. *Arrowheads* and *numbers* to the *right* of each pair of lanes indicate the major cross-link species.

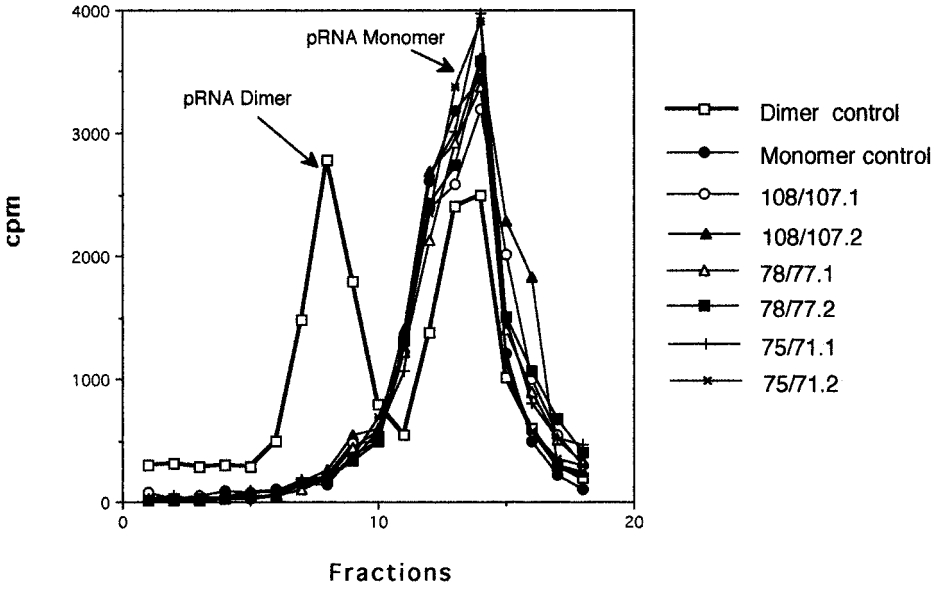

FIG. 3. **Sucrose gradient sedimentation analysis of cross-linked species to determine whether the cross-linking is intra- or intermolecular.** Purified cross-linked conjugates were loaded onto a 5–20% sucrose gradient and sedimented in an ultracentrifuge. All cross-linked samples sedimented identical to monomeric pRNA (monomer) indicating intramolecular cross-linking, while dimeric pRNA complexes (dimer) centered at fraction 8.

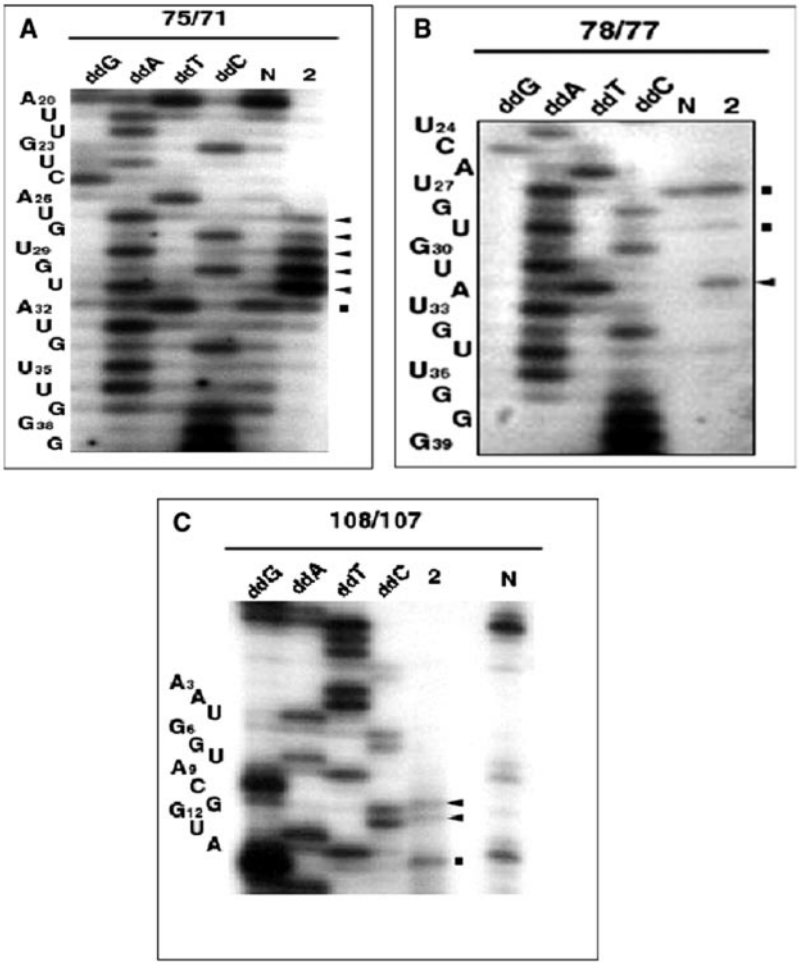

FIG. 4. **Primer-extension mapping of cross-link sites.** Analysis of intramolecular cross-links from cp-pRNA 75/71 (*A*), cp-pRNA 78/77 (*B*), and cp-pRNA 108/107 (*C*). Lanes marked with *ddG*, *ddA*, *ddT*, *ddC*, and *N* denote lanes containing G, A, T, and C sequencing reactions and a control primer extension with noncross-linked RNA, respectively. *Numbered lanes* contain the products of primer-extension reactions using the cross-linked species indicated in Fig. 3. *Arrows* indicate the positions of terminations specific to the cross-linked RNA templates, while *squares* identify nonspecific terminations.

via the azidophenacyl moiety, because unconjugated RNA did not form cross-links (data not shown). The conversion rate of pRNAs containing the photoagent into cross-linked species was 8–18% (Table II). These individual cross-linked species are designated numerically according to their migration rate. For example, the cross-linked species with the slowest and faster migration rate using cp-pRNA 75/71 is denoted apa75-1 and apa75-2, respectively.

Intramolecular cross-linking of 5′APA cp-pRNA results in the formation of lariats, which appear as bands migrating more slowly than uncross-linked RNA in denaturing PAGE. However, it has also been shown recently that pRNA in the presence of Mg^{2+} interacts intermolecularly (24, 25). It was also shown that intermolecular cross-linked pRNAs exhibit slower migration than uncross-linked RNA when resolved on denaturing PAGE (56). Therefore, separation of cross-linked species from noncross-linked RNA by PAGE is insufficient to differentiate between intra- and intermolecular cross-links. To distin-

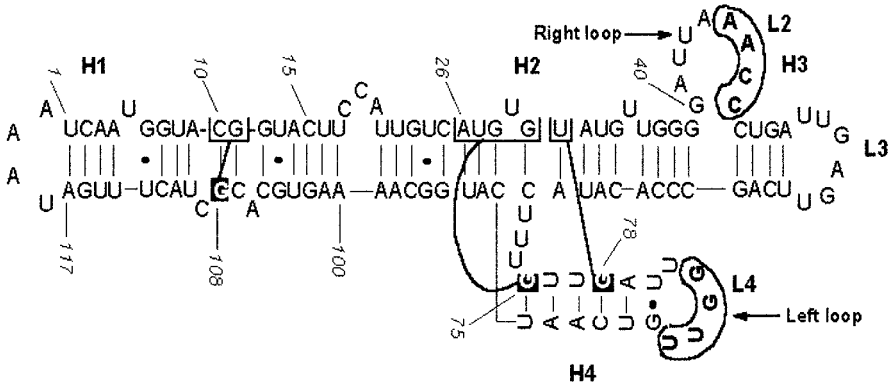

FIG. 5. **Overview of cross-linking results.** Structural constraints from this study are indicated by *lines* to connecting photoaffinity attachment sites (*filled boxes*) and cross-linked bases (*brackets*). The numbering of pRNA is that of the native sequence. Helices are marked and are numbered as they occur 5′ to 3′, *e.g.* helix 3 is the third helix from the 5′-end. The loops of individual helices are marked as *left*, *right*, and head (*H*) loops. The four bases in the *right* and *left loops* responsible for inter-RNA interactions are *boxed* and in *bold*.

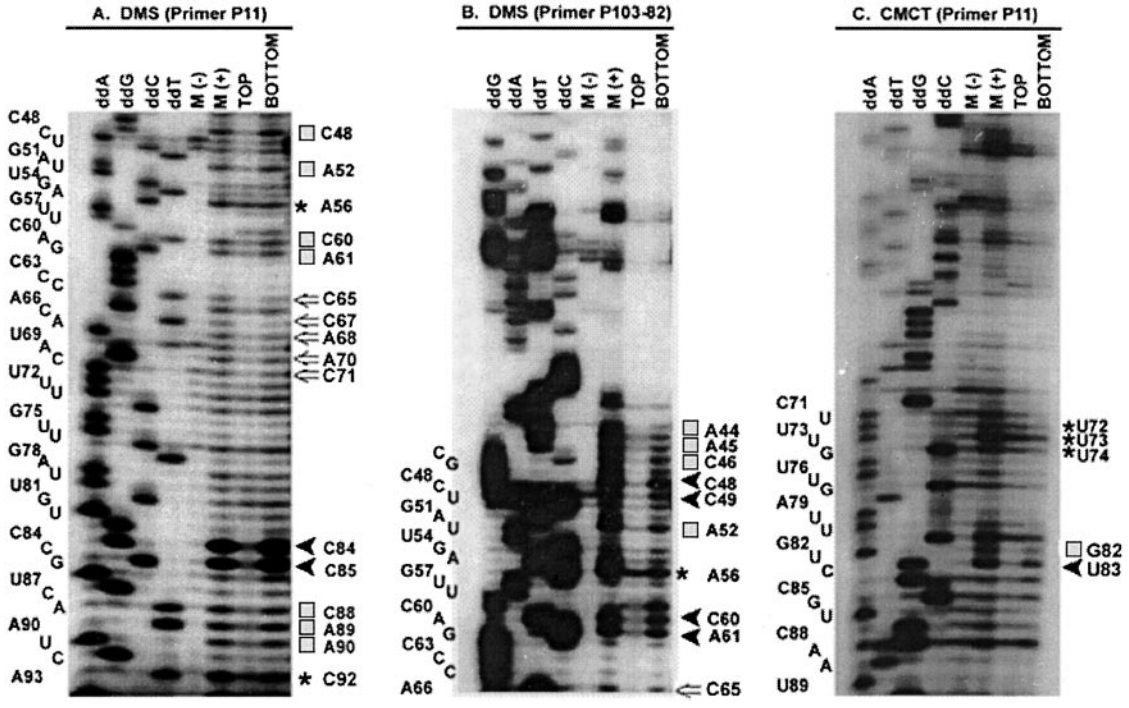

FIG. 6. **Chemical modification interference with DMS and CMCT.** *A*, DMS with primer P11; *B*, DMS with primer P103–82; and *C*, CMCT with primer P11. Examples of autoradiograms of sequencing type gels of primer extension using γ-^{32}P-end labeled primers are shown. Reverse transcriptase stops one nucleotide prior to modified bases. The *M(−)* and *M(+)* indicate primer extension was performed on unmodified and modified 5′/3′ B-a′ pRNA monomer, respectively. The *top* represents the monomer that escapes the modification and thus produces band shift (dimer). The *bottom* represents the monomer that got modified and thus could not form dimer. The *asterisks* before the base indicate the base is not involved in dimerization. The *black arrow* indicates a strong modification, the *gray square* for moderate, and the *double-lined arrow* for weak modification. The *ddA*, *ddG*, *ddC*, or *ddT* indicates that primer extension was performed on unmodified 5′/3′ B-a′ pRNA in the presence of the indicated dideoxynucleoside triphosphate to facilitate precise base mapping. Due to the difficulty in reading extension products of increasing size, only a portion of the gels are shown, thus no full-length products are presented in these figures. Please note that DMS modifies only A and C, while CMCT modifies only U and G. The bases modified unspecifically in both top and bottom are not marked.

guish between intra- and intermolecular cross-links, cross-link species were isolated and subjected to sedimentation through a 5–20% sucrose gradient not containing Mg^{2+}. In such a gradient, intramolecular cross-links will sediment like that of monomeric pRNA, while intermolecular cross-links will sediment like that of multimeric pRNA complexes. From the results shown in Fig. 3, it is clear that all cross-links obtained in this study sedimented identically to the monomer control and thus represents intramolecular cross-links.

Additionally, the formation of intramolecular cross-links was tested by assessing the sensitivity of the reaction to dilution. A dilution of photoagent-modified RNA before UV irradiation would cause a decrease in intermolecular cross-linking rates, whereas intramolecular cross-links should remain unaffected. Dilution up to 100-fold before UV irradiation of cross-linking reactions containing 5′-APA cp-pRNAs did not affect the efficiency of formation of the cross-linked species (data not shown) and implied that the cross-linking is intramolecular rather than intermolecular.

Analysis of Intra-pRNA Cross-linking Sites—The particular nucleotides cross-linked to the modified termini of the cp-pRNAs were determined by primer extension. Individual intramolecular cross-linked species were gel-purified and used as templates for primer extension with reverse transcriptase. Reverse transcriptase terminates one nucleotide 3′ to cross-link sites in the RNA template (57–60). Examples of this analysis for the cross-linked species, derived from apa75-2, apa78-2, and apa108-2 are shown in Fig. 4. Extension products from cross-linked cp-pRNA were compared with that from noncross-linked cp-pRNA to identify the individual cross-linked nucleotides. For intramolecular cross-linked conjugates (apa75-1, apa78-1, and apa108-1), the cross-link sites were apparently located

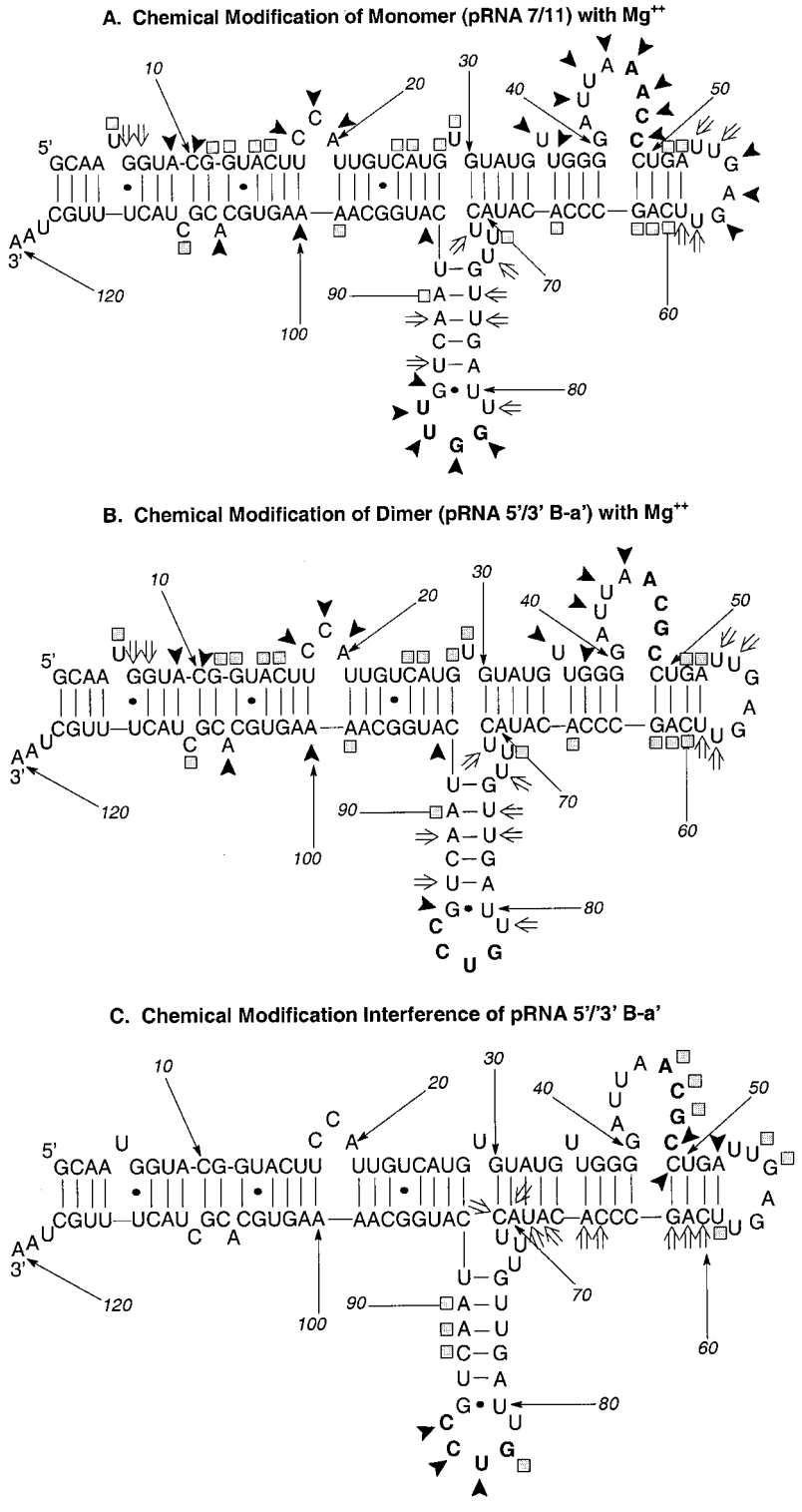

FIG. 7. **Summary of modification interference on pRNA 5′/3′ B-a′ (*C*).** The *black arrow*, *gray square*, and *double-lined arrow* indicate a strong, moderate, and weak modification, respectively. *A* and *B* summarized the chemical modification of monomer and dimer as a comparison (27).

near the 3′-end of the cp-pRNA, within the oligonucleotide primer binding site, and so could not be mapped by primer extension. Table II lists the sites of cross-linking in the species analyzed in this study. The spatial distribution of the related helix is illustrated in Fig. 5 and will be further discussed below.

Procapsid Binding and DNA Packaging Activity of Intramolecular Cross-linked Monomers—To test for the ability of cross-linked cp-pRNA to bind procapsids, intramolecular cross-linked species were gel-purified and incubated with purified procapsids in the presence of Mg^{2+}. Control reactions containing noncross-linked cp-pRNA incubated with purified procapsids and Mg^{2+} were also performed. The cp-pRNA-enriched procapsid complexes were sedimented through sucrose gradients, and procapsid binding efficiencies were determined (Table II). The gel-purified intramolecular cross-link species retain substantial procapsid binding activity.

To analyze the DNA packaging activity, intramolecular cross-links were gel-purified and utilized in *in vitro* phi29 assembly (48, 49). Under identical conditions to those used in assessing the DNA packaging activity of uncross-linked cp-pRNAs, intramolecular cross-links showed reduced activity with respect to their uncross-linked counterparts. Although intramolecular cross-links exhibited relatively poor retention of DNA packaging activity, cp-pRNA cross-links retained good

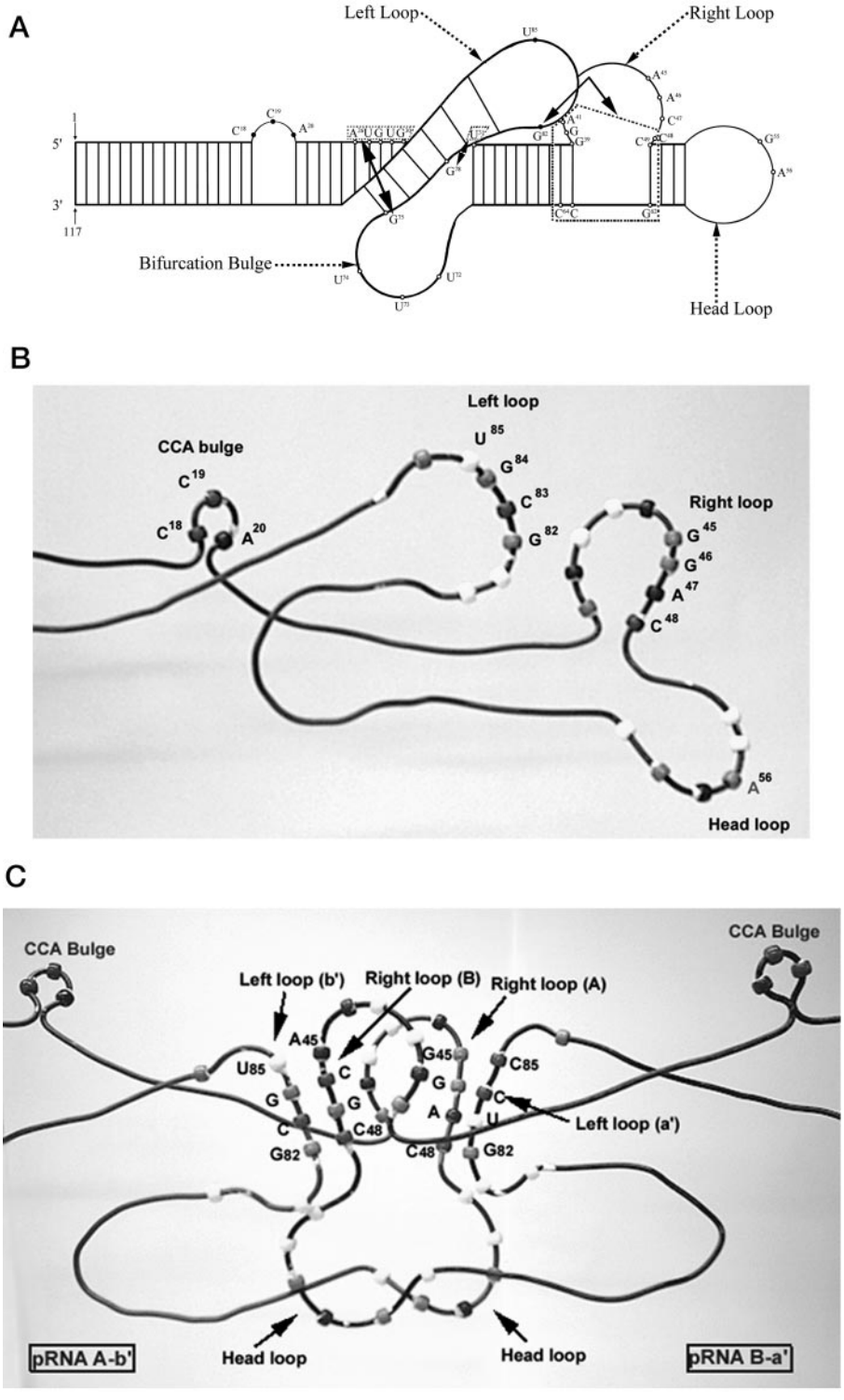

FIG. 8. *A*, Sketch identifies the intramolecular cross-linking sites (identified by a *line* with *double arrowheads*) between base G^{75} to stretch of $A^{26}U^{27}G^{28}U^{29}G^{30}$ and between G^{78} to U^{31}. The flexibility of the bifurcation bulge ($U^{74}U^{73}U^{72}$) at the three-way junction facilitates the flipping of the left loop. Also shown in the sketch is an intermolecular cross-linking between base G^{82} to bases $A^{41}G^{40}G^{39}C^{49}G^{62}C^{63}C^{64}$ (56). *B*, a bead-and-wire model to illustrate pRNA A/b′ monomer. *C*, a bead-and-wire model to illustrate pRNA dimer A/b′-B/a′, based on the data of chemical interference and the cross-linking experiments.

procapsid binding efficiencies (Table II).

Probing the Structure of Dimer by Chemical Modification Interference—Previous work has identified the intermolecular interaction between the right loop of one RNA molecule and the left loop of another RNA molecule (24, 25, 61). This intermolecular interaction between the loops for the formation of a hexamer was refereed as "hand-in-hand" interaction (41). In addition, pRNA dimer has been shown to be the building block for the formation of the hexameric complex. However, the exact pathway of the hexamer formation is still a mystery even though a model has been proposed (26).

To facilitate description of mutant RNAs, we use upper and lowercase letters to represent sequences of the interacting right and left loop (Fig. 1). The same letters in upper and lowercases indicate complementary sequences, while different letters indicate noncomplementary loops. For example, pRNA A-a′ represents a pRNA with complementary right loop A (5′-GGAC[48]) and left loop a′ (3′-CCUG[82]), while pRNA A-b′ represents a pRNA with unpaired right loop A and left loop b′ (3′-UGCG[82]). Dimeric pRNA was produced via intermolecular interaction of the engineered mutant pRNA A-b′ and B-a′. All pRNAs used were circularly permuted pRNA 75/71 (40, 55) with G^{75} and C^{71} as new 5′ and 3′ ends, respectively, except when indicated otherwise.

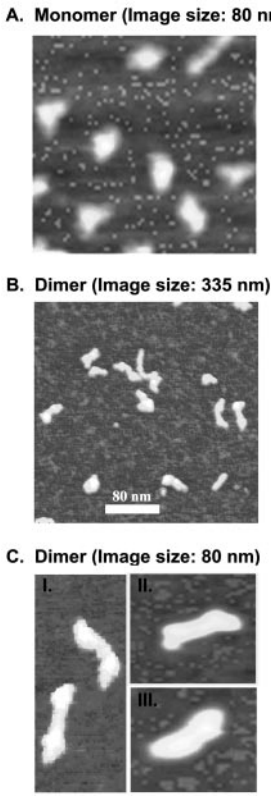

FIG. 9. **Cryo-AFM to compare the covalently linked (fused) dimers (*B* and *C*, *panel I*) with noncovalently linked native dimer (*C*, *panel II* and *C*, *panel III*) of pRNA.** pRNA monomers are also shown in *A*. The striking similarity between the covalently fused pRNA dimer and the native pRNA dimer is uncanny, albeit the covalently linked dimer is slightly thinner at the center. The size of the dimer is about twice the size of the monomer (compare *A* and *C*).

To avoid ambiguities in primer annealing during primer extension, we employed two pRNAs, a regular 120-base, pRNA 5′/3′ B-a′, and a truncated version of the 75-base, 23/97 A-b′. Previously we have shown that 23/97 A-b′ is the smallest molecule competent in forming dimer (41). The 120-base 5′/3′ B-a′ was treated with either DMS or CMCT and then mixed with the 75-base 23/97 A-b′ for dimer formation. The concentration of the chemical is titrated to ensure that on the average only one base is modified for each pRNA. Monomer and dimer were separated and purified from native PAGE. If the modified base is involved in dimer formation, pRNA 5′/3′ B-a′ carrying this modified base would not be able to form dimer with 23/97 A-b′ and thus would stay as the bottom band (monomer). The two bands representing either monomer or dimer were isolated and subjected to primer extension to identify the modified bases. Both primers used for reverse transcriptase are specific to 5′/3′ B-a′ but are not able to bind 23/97 A-b′ to avoid ambiguous results in primer extension.

Examples of autoradiograms of chemical modification interference by both primer P11 and P103-82 are shown in Fig. 6, *A–C*. Reverse transcriptase stops one nucleotide prior to the site of modification. Nonspecific nicks in the RNA or nonspecific stops or pauses in primer extension caused by strong pRNA secondary structure were identified by comparing the primer extension on unmodified 5′/3′ B-a′ monomer as control.

Bases C^{85} and C^{84} showed a very strong involvement in dimer formation as seen by the intensity of the bands. Bases A^{90}, A^{89}, C^{88}, U^{59}, G^{55}, and U^{54} show moderate involvement in dimerization. Bases C^{71}, A^{70}, U^{69}, A^{68}, A^{66}, and C^{65} show weak involvement in dimerization.

In general, bases on the left-hand side of the left loops and bases on the right-hand side of the right loop seem to hold the pRNAs together to form the dimer, as summarized in Fig. 7, *B* and *C*. A series of U^{74}, U^{73}, U^{72} at the bifurcation bulge does not seem to be involved in dimer formation. We believe this bulge provides the flexible hinge for the pRNA to fold.

Integration of Probing Data from Both Monomer and Dimer Concerning pRNA Structure—Data from the photoaffinity cross-link of monomer revealed that base 75 was cross-linked to bases 26–30, and base 78 was cross-linked to base 31. Data from chemical modification revealed that bases 75–80 and bases 30–34 were protected from modification by chemicals (27). Chemical modification interference revealed that bases 72–81 were not involved in dimer formation. Therefore, it is concluded that bases 75–81 and bases 31–35 are proximate. The 9-Å cross-linking distance imposed by the photoaffinity agent allows the nucleotides to cross-link to bases three to four bases away in the sequence. Interaction between sequences 75–81 and 31–35 will produce a pocket for RNA-RNA interaction in dimer formation. Chemical modification interference revealed that bases 45–71 and 82–91 were involved in dimer formation. Fig. 8, *A* and *C*, illustrates the interaction that might have taken place in pRNA dimer.

Cryo-AFM Images of Covalently Linked Dimers—We have reported that the covalently linked dimeric pRNA is active in phi29 DNA packaging (26). It is interesting to find out whether the overall structure of the covalently linked dimer is similar to the native pRNA dimer formed through hand-in-hand interaction.

We used the cryo-AFM to directly visualize purified pRNA monomers and dimers. Previously, we report the pRNA monomer (27) (Fig. 9*A*) folded into a "✔"-shaped structure, while dimers of A-b′/B-a′ complex have an elongated shape (Fig. 9, *B* and *C*). The overall length of a monomer was found to be 16.7 ± 0.9 nm. The dimer had a length of 30.2 ± 2.5 nm with a width of 11.6 ± 1.4 nm (27). Since the dimer is elongated, it appears that head to head contact was involved in dimer formation, resulting in a complex almost twice as long as a monomer. It was also shown that nucleotides of the head loop in dimers were protected from chemical attacks, strongly supporting a head to head contact in dimer formation, in addition to right and left loop interaction. Cryo-AFM images of the fused dimer (Fig. 9, *B* and *C–I*) exhibit a similar structure to the noncovalently linked pRNA dimer (Fig. 9C, *panels II* and *III*). The dimensions of the covalently linked fused dimer are comparable with the previously reported dimer (26, 27).

DISCUSSION

Intramolecular cross-links exhibited relatively poor retention of DNA packaging activity; cp-pRNA cross-links retained good procapsid binding efficiencies (Table II). Thus, poor DNA packaging activities exhibited by the intramolecular cross-linked species probably is due to the loss of flexibility after cross-link. It is expected that conformation change of pRNA is needed during the DNA translocation process (20).

Although the mechanism of phi29 pRNA dimer formation is similar to that of the kissing loop of HIV, the type of loop-loop interaction of phi29 pRNA is in some respects different from pseudoknots (62, 63) and kissing loops (64–68). Pseudoknots involve the intramolecular interactions within one single molecule. Kissing loops involve the interaction of two self-complementary loops to form a dimer (69, 70). Since phi29 pRNA form closed hexameric rings, the intermolecular interaction of pRNA must require that each RNA molecule contribute one loop to pair with the alternate loop of the next pRNA, as shown in Fig. 8. The key feature in the "hand-in-hand model" is that multiple RNAs interact via alternate interlocking loops to form a closed

ring, while interaction of kissing loops refers to the formation of dimers, not rings.

Such hand-in-hand loop-loop interactions may also play an important role in other systems as well. For example, RNA-RNA interaction via alternating loops has also been reported for *bicoid* mRNA in *Drosophila* embryos (38). We speculated that the mechanism of *bicoid* mRNA interaction and translocation might be similar to that of phi29 pRNA (41). It is possible, although not proven, that a *bicoid* mRNA may also form multimeric rings to ride, track, or rotate along Staufen protein during its transportation. Indeed, there is evidence that *bicoid* mRNA can form multimers (Fig. 3 of Ref. 38).

Hand-in-hand interaction is the mechanism in pRNA hexamer formation (24, 41). The pRNA dimer reported here also involved hand-in-hand interaction. In dimer, each pRNA only held hands of "one" additional pRNA. However, in hexamers, each pRNA held hands of "two" additional pRNAs. It seems paradoxical concerning the hand interaction in dimer and hexamer. How to interpret the conclusion that dimer is the building block for pRNA hexamer? We found that the pRNA has a strong tendency to form a circular ring by hand-in-hand contact regardless of dimer, trimer, or hexamer.[2] Therefore, a conformational shift is expected during the transition from dimer to hexamer. We speculate that dimer formation is a prerequisite to generate an appropriate three-dimensional interface for procapsid binding. One of the hands of the dimer would release after binding to the procapsid. The dimer with a released hand is similar to the open (linear) dimer that has been demonstrated to be unstable in solution but was still active in procapsid binding and DNA packaging (41). The release hand will serve as a welcoming hand to recruit the incoming dimer. Such conformation shift could be the intrinsic nature of such intriguing RNA that could bear the moving task in DNA transportation.

Acknowledgments—We thank Stephen Hoeprich and Dan Shu for their help in preparing this manuscript and Dr. David Williams for the drawing of Fig. 8*A*.

REFERENCES

1. Greatorex, J. S., Laisse, V., Dokhelar, M. C., and Lever, A. M. L. (1996) *Nucleic Acids Res.* **24,** 2919–2923
2. Skripkin, E., Paillart, J. C., Marquet, R., Ehresmann, B., and Ehresmann, C. (1994) *Proc. Natl. Acad. Sci. U. S. A.* **91,** 4945–4949
3. Berglund, J. A., Abovich, N., and Rosbash, M. (1998) *Genes Dev.* **12,** 858–867
4. Verma, M., Kurl, R. N., Blass, C., and Davidson, E. A. (1997) *Cancer Biochem. Biophys.* **15,** 211–220
5. Valcarcel, J., Gaur, R. K., Singh, R., and Green, M. R. (1996) *Science* **273,** 1706–1709
6. Sontheimer, E. J., and Steitz, J. A. (1993) *Science* **262,** 1989–1996
7. Guerrier-Takada, C., Gardiner, K., Marsh, T., Pace, N., and Altman, S. (1983) *Cell* **35,** 849–857
8. Oh, B. K., and Pace, N. R. (1994) *Nucleic Acids Res.* **22,** 4087–4094
9. Baer, M. F., Reilly, R. M., McCorkle, G. M., Hai, T. Y., Altman, S., and RajBhandary, U. L. (1988) *J. Biol. Chem.* **263,** 2344–2351
10. Henkin, T. M. (1996) *Annu. Rev. Genet.* **30,** 35–57
11. Lease, R. A., Cusick, M. E., and Belfort, M. (1999) *Proc. Natl. Acad. Sci. U. S. A.* **95,** 12456–12461
12. Moss, E. G., Lee, R. C., and Ambros, V. (1997) *Cell* **88,** 637–646
13. Jorgensen, R. A., Atkinson, R. G., Forster, R. L., and Lucas, W. J. (1998) *Science* **279,** 1486–1487
14. Panning, B., and Jaenisch, R. (1998) *Cell* **93,** 305–308
15. Eguchi, Y., and Tomizawa, J. (1990) *Cell* **60,** 199–209
16. Guo, P., and Trottier, M. (1994) *Semin. Virol.* **5,** 27–37
17. Guo, P., Erickson, S., and Anderson, D. (1987) *Science* **236,** 690–694
18. Guo, P., Bailey, S., Bodley, J. W., and Anderson, D. (1987) *Nucleic Acids Res.* **15,** 7081–7090
19. Garver, K., and Guo, P. (1997) *RNA* (*N. Y.*) **3,** 1068–1079
20. Chen, C., and Guo, P. (1997) *J. Virol.* **71,** 3864–3871
21. Trottier, M., and Guo, P. (1997) *J. Virol.* **71,** 487–494
22. Chen, C., Trottier, M., and Guo, P. (1997) *Nucleic Acids Symp. Ser.* **36,** 190–193
23. Trottier, M., Zhang, C. L., and Guo, P. (1996) *J. Virol.* **70,** 55–61
24. Guo, P., Zhang, C., Chen, C., Trottier, M., and Garver, K. (1998) *Mol. Cell* **2,** 149–155
25. Zhang, F., Lemieux, S., Wu, X., St.-Arnaud, S., McMurray, C. T., Major, F., and Anderson, D. (1998) *Mol. Cell* **2,** 141–147
26. Chen, C., Sheng, S., Shao, Z., and Guo, P. (2000) *J. Biol. Chem.* **275,** 17510–17516
27. Trottier, M., Mat-Arip, Y., Zhang, C., Chen, C., Sheng, S., Shao, Z., and Guo, P. (2000) *RNA* (*N. Y.*) **6,** 1257–1266
28. Guo, P., Peterson, C., and Anderson, D. (1987) *J. Mol. Biol.* **197,** 229–236
29. Young, M. C., Schultz, D. E., Ring, D., and von Hippel, P. H. (1994) *J. Mol. Biol.* **235,** 1447–1458
30. Doering, C., Ermentrout, B., and Oster, G. (1995) *Biophys. J.* **69,** 2256–2267
31. Young, M., Kuhl, S., and von Hippel, P. (1994) *J. Mol. Biol.* **235,** 1436–1446
32. West, S. C. (1996) *Cell* **86,** 177–180
33. Egelman, E. H. (1996) *Structure* (*Lond.*) **4,** 759–762
34. San Martin, M. C., Gruss, C., and Carazo, J. M. (1997) *J. Mol. Biol.* **268,** 15–20
35. Herendeen, D. R., Kassavetis, G. A., and Geiduschek, E. P. (1992) *Science* **256,** 1298–1303
36. Geiselmann, J., Wang, Y., Seifried, S. E., and von Hippel, P. H. (1993) *Proc. Natl. Acad. Sci. U. S. A.* **90,** 7754–7758
37. Geiduschek, E. P. (1997) *Chem. Biol.* **2,** 123–125
38. Ferrandon, D., Koch, I., Westhof, E., and Nusslein-Volhard, C. (1997) *EMBO J.* **16,** 1751–1758
39. Zhang, C. L., Lee, C.-S., and Guo, P. (1994) *Virology* **201,** 77–85
40. Zhang, C. L., Trottier, M., and Guo, P. X. (1995) *Virology* **207,** 442–451
41. Chen, C., Zhang, C., and Guo, P. (1999) *RNA* (*N. Y.*) **5,** 805–818
42. Zuker, M. (1989) *Science* **244,** 48–52
43. Moazed, U., Stern, S., and Noller, H. F. (1986) *J. Mol. Biol.* **187,** 399–416
44. Burgin, A. B., and Pace, N. R. (1990) *EMBO J.* **9,** 4111–4118
45. Guo, P., Rajogopal, B., Anderson, D., Erickson, S., and Lee, C.-S. (1991) *Virology* **185,** 395–400
46. Guo, P., Erickson, S., Xu, W., Olson, N., Baker, T. S., and Anderson, D. (1991) *Virology* **183,** 366–373
47. Salas, M. (1991) *Annu. Rev. Biochem.* **60,** 39–71
48. Lee, C. S., and Guo, P. (1994) *Virology* **202,** 1039–1042
49. Lee, C. S., and Guo, P. (1995) *J. Virol.* **69,** 5018–5023
50. Guo, P., Grimes, S., and Anderson, D. (1986) *Proc. Natl. Acad. Sci. U. S. A.* **83,** 3505–3509
51. Han, W., Mou, J., Sheng, J., Yang, J., and Shao, Z. (1995) *Biochemistry* **34,** 8215–8220
52. Zhang, Y., Sheng, S., and Shao, Z. (1996) *Biophys. J.* **71,** 2168–2176
53. Pan, T., Gutell, R. R., and Uhlenbeck, O. C. (1991) *Science* **254,** 1361–1364
54. Nolan, J. M., Burke, D. H., and Pace, N. R. (1993) *Science* **261,** 762–765
55. Zhang, C. L., Tellinghuisen, T., and Guo, P. (1997) *RNA* (*N. Y.*) **3,** 315–322
56. Garver, K., and Guo, P. (2000) *J. Biol. Chem.* **275,** 2817–2824
57. Hagenbuchle, O., Santer, M., and Steitz, J. A. (1978) *Cell* **13,** 551–563
58. Youvan, D. C., and Hearst, J. E. (1982) *Anal. Biochem.* **119,** 86–89
59. Barta, A., Steiner, G., Brosius, J., Noller, H. F., and Kuechler, E. (1984) *Proc. Natl. Acad. Sci. U. S. A.* **81,** 3607–3611
60. Inoue, T., and Cech, T. R. (1985) *Proc. Natl. Acad. Sci. U. S. A.* **82,** 648–652
61. Hendrix, R. W. (1998) *Cell* **94,** 147–150
62. Pleij, C. W. A., and Bosch, L. (1989) *Methods Enzymol.* **180,** 289–303
63. Studnicka, G. M., Rahn, G. M., Cummings, I. W., and Salser, W. A. (1978) *Nucleic Acids Res.* **5,** 3365–3387
64. Paillart, J. C., Skripkin, E., Ehresmann, B., Ehresmann, C., and Marquet, R. (1996) *Proc. Natl. Acad. Sci. U. S. A.* **93,** 5572–5577
65. Prats, A. C., Roy, C., Wang, P. A., Erard, M., Housset, V., Gabus, C., Paoletti, C., and Darlix, J. L. (1990) *J. Virol.* **64,** 774–783
66. Bender, W., and Davidson, N. (1976) *Cell* **7,** 595–607
67. Chang, K. Y., and Tinoco, I., Jr. (1997) *J. Mol. Biol.* **269,** 52–66
68. Laughrea, M., Jette, L., Mak, J., Kleiman, L., Liang, C., and Wainberg, M. A. (1997) *J. Virol.* **71,** 3397–3406
69. Homann, M., Rittner, K., and Sczakiel, G. (1993) *J. Mol. Biol.* **233,** 7–15
70. Clever, J. L., Wong, M. L., and Parslow, T. G. (1996) *J. Virol.* **70,** 5902–5908
71. Wichitwechkarn, J., Bailey, S., Wodley, J. W., and Anderson, D. (1989) *Nucleic Acids Res.* **17,** 3459–3468
72. Siebenlist, A., Simpson, R. B., and Gilbert, W. (1980) *Cell* **20,** 269–281

[2] D. Shu and P. Guo, unpublished results.